Colloid Polym Sci (2006) 285:283–292
DOI 10.1007/s00396-006-1562-z

ORIGINAL CONTRIBUTION

In situ metal particle preparation in cross-linked poly (2-acrylamido-2-methyl-1-propansulfonic acid) hydrogel networks

Nurettin Sahiner

Received: 26 June 2006 / Accepted: 7 August 2006 / Published online: 17 October 2006

Abstract Anionic hydrogels of poly(2-acrylamido-2-methyl-1-propansulfonic acid) (p(AMPS)) were prepared with a different amount of cross-linker extent and used for in situ preparation of magnetic and metal particles. The metal particles with various sizes were obtained inside the three-dimensional polymer matrixes by absorption of the corresponding metal ions from their aqueous solutions followed by the reduction in the presence of strong reducing agent. In addition to iron particles, cobalt, nickel, copper nanoparticles, and CdS, quantum dot has been prepared by utilizing hydrogel matrix as a template for inorganic/organic composite synthesis. It was observed that the amount of cross-linkers (0.5%, 0.75%, and 1% with respect to monomer mole ratio) used in this study for bare p(AMPS) has not significantly influenced the morphology of the hydrogels or the size of the iron particles while having great effect on swelling of p(AMPS) hydrogels in water. Copolymeric hydrogels of AMPS with acrylamide in different composition were also prepared. Thermogravimetric analysis and transmission electron microscopy results showed that the AMPS content of the copolymeric hydrogel has great impact on both the metal ion loading capacity and the size of the resultant metal particles.

N. Sahiner (✉)
Chemical and Biomolecular Engineering, Tulane University,
300 Lindy Boggs Bldg,
New Orleans, LA 70118, USA
e-mail: sahiner@udel.edu

Present address:
N. Sahiner
Deparment of Chemistry, Canakkale Onsekiz Mart University,
Terzioglu Campus,
Canakkale, 17020, Turkey

Keywords Nanoparticle · Nanocomposites · Magnetic field sensitive hydrogels

Introduction

Material synthesis in geometrically constrained area is well established and very important for the resultant material in terms of their physical and chemical properties. Surfactants [1], block copolymers [2], multilayers of sequentially adsorbed polyelectrolytes [3] or layer-by-layer polyionic assemblies [4, 5], and polymeric micelles including reverse micelles [6] are among the widely used confined environments for novel material synthesis [7]. Polymeric gels have been developed in the last couple of decades, are diverse, and have unique properties that make them scientifically important materials [8–10]. The intrinsic characteristics of hydrogels such as elasticity, porosity, and water retention ability make them essential in many applications as scaffolds in cell-growing media and tissue engineering as well as for the fabrication of three-dimensional bonelike composites by template-driven mineralization technique [11, 12]. Hydrogel networks can offer interesting environment for nanoparticle synthesis for many applications [13, 14]. Due to the potential applications of magnetic gels in magnetic drug delivery, cell sorting, catalysis, sensor, and actuators, there has been a lot of research focused on magnetic composite material synthesis [15, 16]. Shipway and Willner [17] suggested that cross-linking of nanoparticles with molecular receptors yields conductive arrays with specific recognition features and controllable porosity, and the integration of the nanoparticles with polymeric hydrogels facilitates the ways to design signal-triggered materials with novel electronic properties. The application

of these types of materials ranges from information storage [7, 18] to hyperthermia applications [19].

A ferrogel is a polymeric gel that imbibes ferromagnetic fluid or finely distributed ferromagnetic particles, which are attached to the flexible network chains by adhesive forces giving rise to direct coupling between the magnetic and mechanical properties. If the cross-linked polymer networks swollen by ferrofluid of colloidal dispersion of monosized magnetic particle with a typical size of roughly 10 nm (below 7 nm), the magnetization of ferreogel is superparamagnetic [20], which is the same as of ferromagnetic fluids. On the other hand, if the diameter of the particle is larger than about 100 nm, the magnetism of the magnetic gel corresponds to ferromagnetism [21]. To prepare organic/inorganic composite materials, generally two methods are employed: one of which is the synthesis of inorganic and polymeric materials separately followed by their combination via grafting or adsorption of polymer chains onto an inorganic core or vice versa [22–24]. The second method is the ion exchange between the counter ions in the electric double layer of the latex microbeads and metal ions followed by treatment with suitable chemicals for nanoparticle formation [25]. Here, an approach is described by utilizing three-dimensional network of functional hydrogel for in situ formation of iron/metal particles inside the polymer matrix. A similar work was recently demonstrated for the preparation of semiconductor nanoparticles in the constrained geometry of polymer microgels composed of a terpolymer of *N*-isopropylacrylamide, acrylic acid, and 2-hydroxyethylacrylate [26]. However, in this work, a pH-sensitive poly(2-acrylamido-2-methyl-1-propansulfonic acid) (p(AMPS)) hydrogels with strong ion exchange capability were employed for metal fabrication inside the three-dimensional hydrogel network for the synthesis of composite materials. It was shown that p(AMPS) network can be used not just for the in situ synthesis of iron particles but also for the other kinds of metal particles such as copper, cobalt, nickel, and their alloys and even cadmium sulfides as quantum dots. Initially, iron ion or different other metal ions were absorbed from their appropriate salt solutions into the preformed polymer network by utilizing ion exchange ability of pH-sensitive hydrogel. Then, the metal ion-loaded networks were treated with a reducing agent. The effects of cross-linking density of the template and copolymeric compositions on the inorganic particle sizes and on the metal loading capacities were investigated.

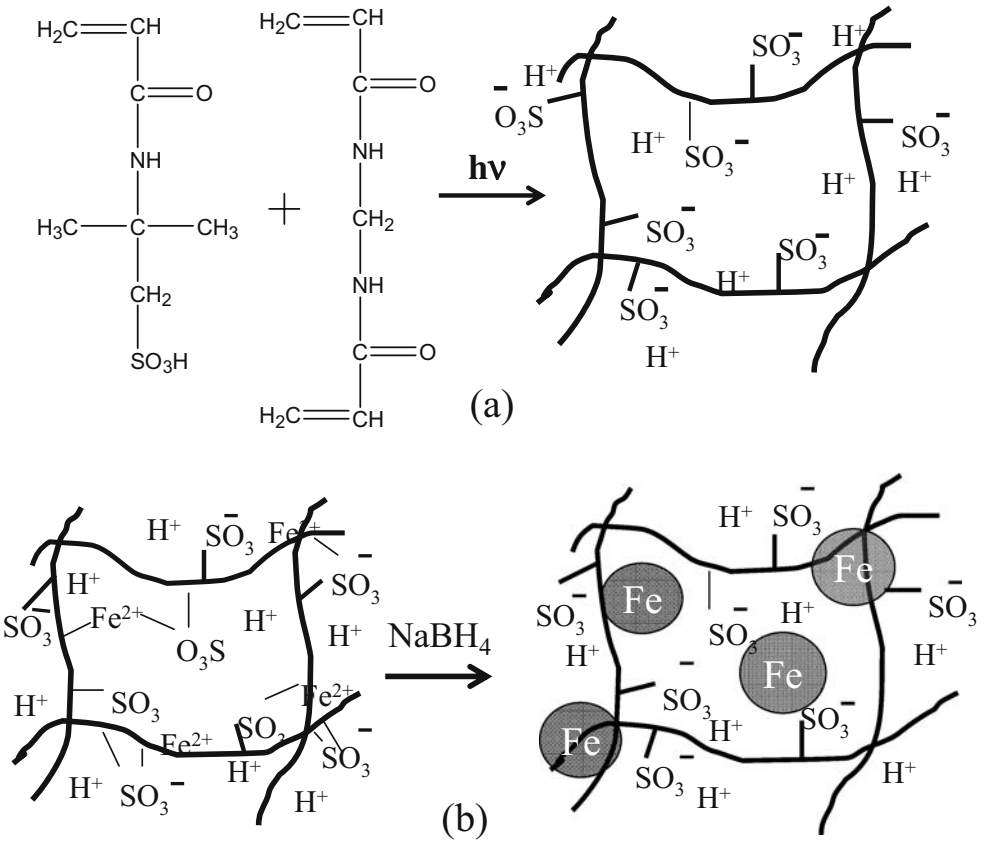

Fig. 1 Schematic of p(AMPS) synthesis mechanism (**a**) and iron particle formation inside p(AMPS) hydrogel (**b**)

Experimental

Materials

For hydrogel synthesis, 2-acrylamido-2-methyl-1-propansulfonic acid (AMPS) and acrylamide (AAm) as monomers and *N*,*N*′-methylenebisacrylamide (Bis) as a cross-linker (X) were used. $FeSO_4 \cdot 7H_2O$ (0.5 M), $CuCl_2 \cdot 2H_2O$ (0.1 M), $CoCl_2 \cdot 6H_2O$ (0.1 M), and $NiCl_2 \cdot 6H_2O$ (0.1 M) as metal ion source and $NaBH_4$ as reducing agent were used for in situ iron and metal particle formation. All the reagents were of analytical grade or highest purity available, used without further purification, and purchased from Aldrich Chemical Company, Inc. (Milwaukee, WI).

Hydrogel synthesis

Cross-linked p(AMPS) hydrogel was prepared by employing UV irradiation of aqueous solution of AMPS monomer containing different amounts of Bis with respect to monomer ratios. Three different percent cross-linked hydrogels, that is, 1%, 0.75%, and 0.5%, were prepared. In typical hydrogel synthesis, 4 g AMPS (0.0193 mol) was mixed with 4 ml distilled water containing various amounts of Bis and vortex mixed until completely transparent solution was obtained. To remove the dissolved oxygen from hydrogel precursors, N_2 was purged from each vial for approximately 1 min. Then, the hydrogel precursor solutions were transferred to one end sealed transparent plastic straws of 0.8-mm inner diameter and irradiated for 2 h. Additionally, copolymeric hydrogels with AAm p(AMPS-c-AAm), that is, AMPS/AAm mole ratio (1.0:0, 0.75:0.25, 0.50:0.50, 0.25:0.75, 0:1.0), were also prepared by the same route at 1% and 0.5% X ratios to the total monomer concentration.

Metal particle formation in the hydrogel network

The prepared different % X p(AMPS) hydrogels were cut into 3- to 5-cm-long cylindrical shape and placed in distilled water to remove the unpolymerized/cross-linked species (cross-linker, monomer, polymer, etc.) from the network for 2 days by replacing the water every 6 h. After the cleaning procedure, the swollen hydrogel particles were transferred into aqueous solutions of 100 ml 0.5 M iron or 0.1 M metal ion containing beakers and kept at ambient temperature in a shaker for 2 days. The amount of hydrogel was adjusted in way that there were always excess amounts of metal ions (e.g., at least four Fe^{2+} ions for every $-SO_3H$ functional group). After completing the absorption of metal ions into p(AMPS) and p(AMPS-c-AAm) hydrogel networks, hydrogels were again washed with distilled water as described above to remove the physisorbed or unbound iron/metal ions for 2 days. The metal ion-loaded hydrogels were finally transferred into a flask containing 100 ml of 0.5 M $NaBH_4$ aqueous solution, and the reduction reaction proceeded for 2 days in a water bath shaker at ambient temperature.

Morphological studies

To investigate the morphology of the p(AMPS) hydrogel, scanning electron microscopy (SEM) (HITACHI High Tech S3000 N) studies were conducted on freeze-dried hydrogels samples. A water-swollen hydrogel disk of 1- to 2-mm thickness placed on aluminum stub before freeze-drying. SEM images were obtained after ~5-nm-thickness gold sputtering with the operating voltage of 10–15 kV. Transmission electron microscopy (TEM; JEOL 2010 TEM) was also employed for the metal particle size determination after finely grinding the dried composite hydrogel particles and placing the powder of hydrogel-metal composites on formwar-coated copper TEM grids. TEM micrographs were acquired at an operating voltage of 200 kV.

Thermal and structural characterization

To determine the amounts of metal loadings and investigate the thermal behavior of all the synthesized hydrogels, thermogravimetric analysis (TGA) was conducted (TGA

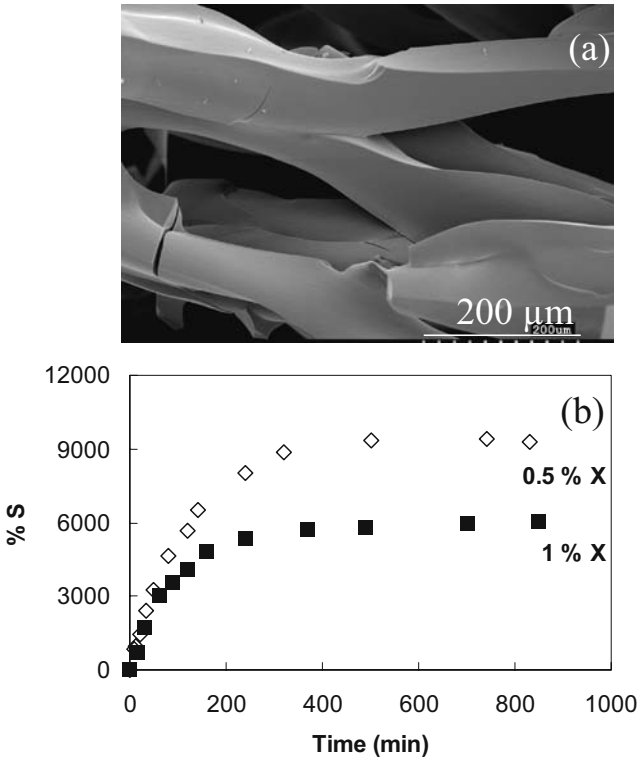

Fig. 2 SEM images of freeze-dried bulk 0.75% cross-linked (X) p(AMPS) (**a**) and swelling behavior of p(AMPS) hydrogel synthesized with different amount of cross-linker (**b**)

Universal V3.7A TA instrument). Freeze-dried or vacuum oven-dried bare hydrogels and iron/metal-loaded hydrogels were crashed into powder form by the aid of mortar and pestle and heated up to 1,000 °C under N_2 or O_2 with 10 °C/min heating rate. For the determination of iron content of hydrogel composites, N_2 gas was chosen to prevent oxidation of metal particles.

Magnetic and crystallographic properties of the synthesized materials were investigated using Vibrating Sample Magnetometer (VSM) and wide-angle X-ray diffraction (XRD) measurements, respectively.

Results and discussion

Composite hydrogel characteristics

After placing water-swollen hydrogel in 0.5 M $FeSO_4$ solution for 2 days, only a slight color change of hydrogels from transparent to very light yellow was observed. Iron and metal ion-loaded hydrogels were washed with distilled water for 2 days to remove excess and unbind and/or physisorbed metal ions from surface and from the interspace/pores of the network. Upon addition of reducing agent, 0.5 M $NaBH_4$ solutions, to iron loaded hydrogels, a dark-green color was formed only on the hydrogel particles with evolution of H_2 gas bubbles from the solution. Depending on the types of metal ion, the color and the intensity varied. The reaction was proceeded for 2 days. Figure 1 depicts the conceptual scheme of (a) hydrogel synthesis and (b) iron particle formation inside p(AMPS). Figure 1b depicts that the iron ions, which were held in place via sulfonyl group electrostatic interactions on the hydrogel network, were reduced with $NaBH_4$. For the morphological investigation of the networks of different % X p(AMPS) hydrogel and its composites, SEM studies were performed on freeze-dried bulk p(AMPS). Figure 2a illustrates SEM images of freeze-dried 0.75% X p(AMPS). It is noteworthy to mention that all the hydrogels showed almost same morphological behaviors regardless of the amount of cross-linker used. Iron-loaded composite-p(AMPS) (c-p(AMPS)) hydrogels were also showed very similar morphology (figure is not shown) with a very small differences in comparison with the smooth texture of p (AMPS) hydrogels. As can be seen from Fig. 2a, p(AMPS) hydogels have very smooth texture with very large pores on the orders of micrometers. For iron particle formation, only 1%, 0.75%, and 0.5% X bulk cylindrical hydrogels were used due to the fragility of the hydrogels with higher cross-linker ratio. Although the swelling of 0.5% X hydrogel is

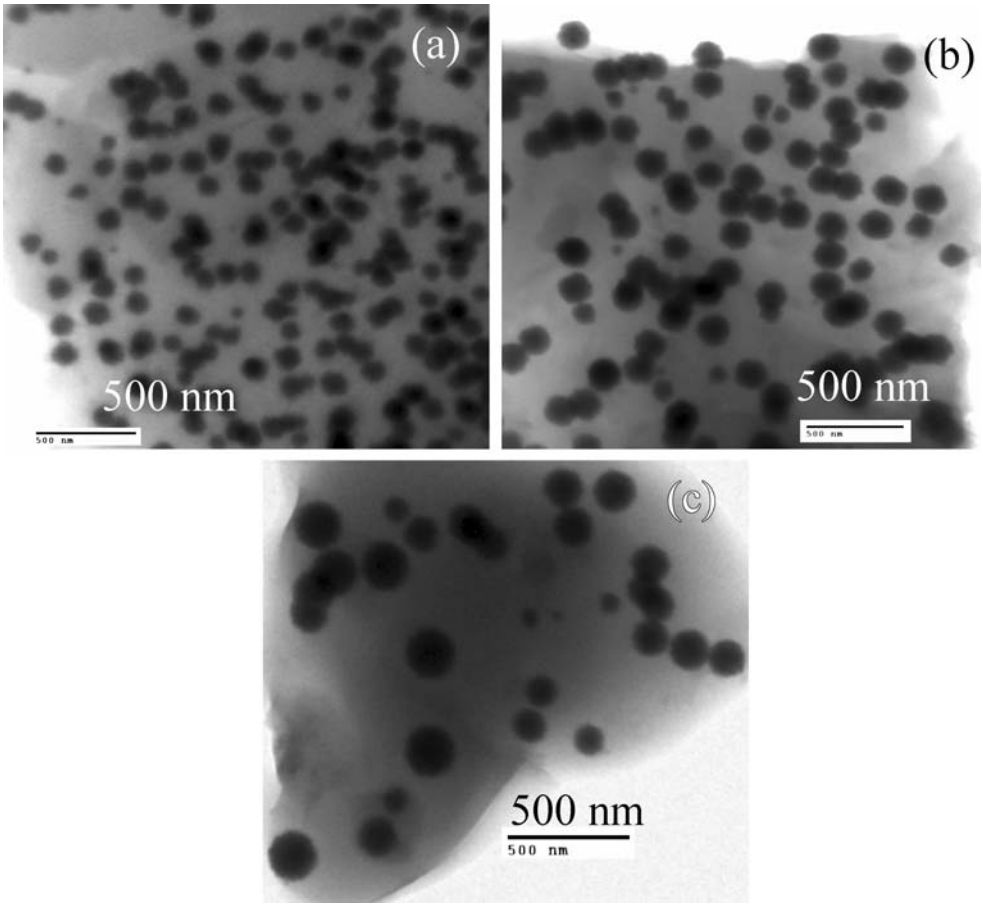

Fig. 3 TEM images of 0.5% (**a**), 0.75% (**b**), and 1% (**c**) X iron particle containing composite-p(AMPS) (c-p(AMPS)) hydrogels

much more than 1% X hydrogels, they have similar characteristic in terms of the iron ion absorption and metal particle formation. Figure 2b is the graph of gravimetric percentage swelling ratio (% S) versus time for 0.5% and 1% X p(AMPS) hydrogels in water. Dried, known amount of hydrogels was placed in distilled water and occasionally removed from the swelling medium for weighing. The increase in weight percent versus time graph is constructed. As can be seen from the figure, the change in the cross-linker amount from 0.5% to 1% almost changes the swelling ratio from ~9,000% to ~6,000%.

Figure 3 depicts the TEM images of different % X c-p (AMPS) hydrogels containing iron particles. All the vacuum oven-dried hydrogel samples were grinded in mortar with pestle and corresponding powders were deposited on formvar-coated copper TEM grids. The sample preparation does not affect the particle size since only hydrogel matrix was crushed into smaller pieces. The TEM images revealed that the iron particles are nearly evenly distributed throughout the network and vary in sizes and almost spherical in shape regardless of cross-linking density of the hydrogels. Roughly homogenous distribution of metal particles inside hydrogels network confirms that Fe^{2+} ions, absorbed by sulfonyl groups, pendant from hydrogel network, were at enough proximity to nucleate iron particles growth upon reaction with $NaBH_4$. The hydrogel of p(AMPS) is homopolymer and every monomer unit carries a sulfonyl functional group which is an ion exchange site for metal ion absorption. Owing to the small extent of cross-linker inside hydrogel (maximum 1 mole% with respect to monomer), the network can be assumed homogenous and sulfonyl groups are evenly distributed along the network. Hence, the iron particles grow almost uniformly from outside of the bulk hydrogel to inward as the diffusion of $NaBH_4$ proceeds with time at this direction. This phenomenon showed itself as dark coloration instantaneously upon contacting iron ion-loaded hydrogels with $NaBH_4$ solution. Initially, a dark-green color was developed from hydrogel particles surface and edges (the outermost skin) and propagated towards inward with time. It is plausible to hypothesize that the metal particles could keep growing using up all the neighboring metal ions available until reaching certain size and stop when no more metal ion is available or exists.

It was found that the cross-linking density is not a limiting parameter with very little or no effect on metal

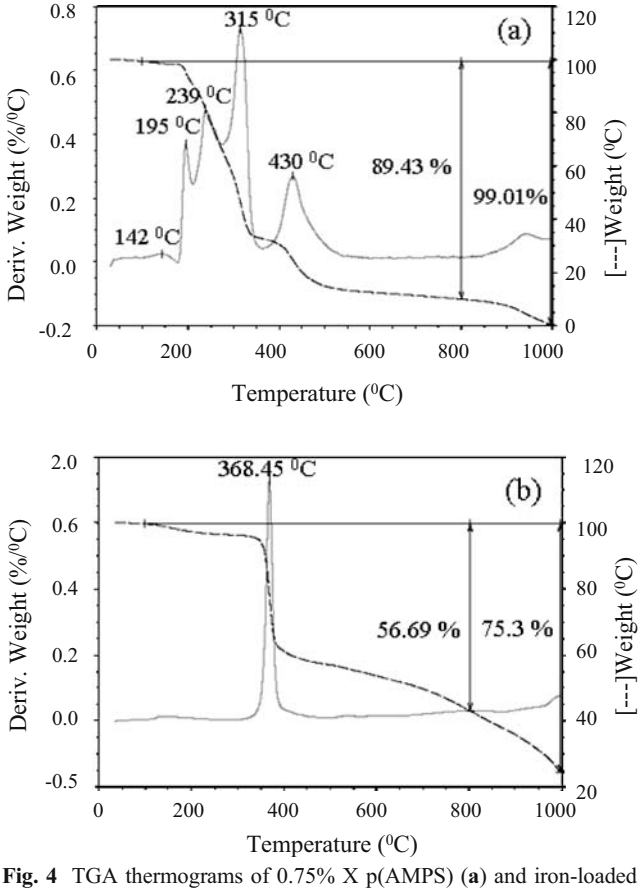

Fig. 4 TGA thermograms of 0.75% X p(AMPS) (**a**) and iron-loaded c-p(AMPS) hydrogels (**b**)

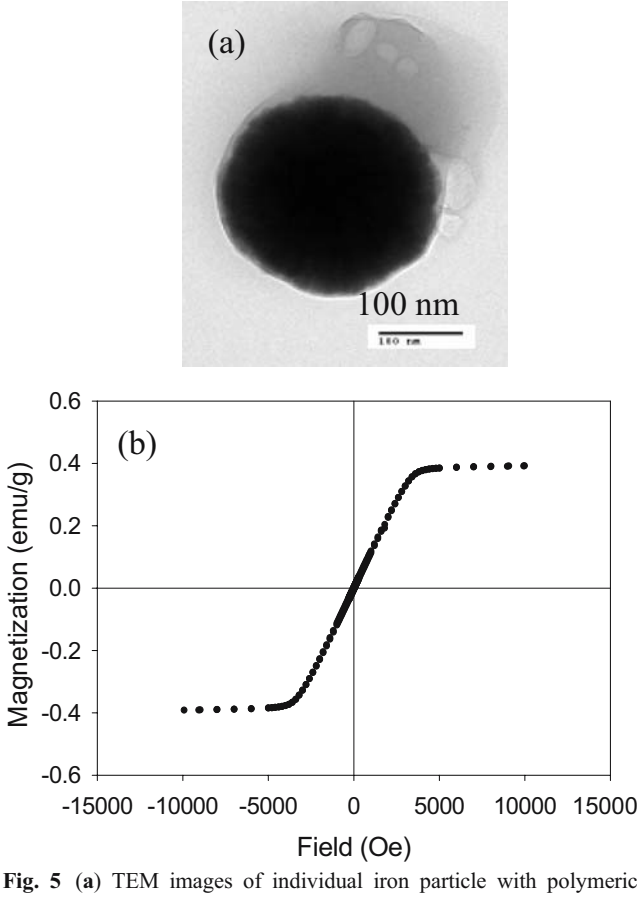

Fig. 5 (**a**) TEM images of individual iron particle with polymeric network. (**b**) Magnetization curve of 0.75 % X c-p(AMPS) hydrogel at room temperature

particle formation in the studied interval. Since this work is in situ metal particle synthesis, it also investigated the extent of ligands on particle size distribution and loading capacity. For this purpose, copolymeric hydrogels with different amounts of AMPS content were prepared. AAm was chosen as a comonomer because it is neutral and has the same repeating unit as AMPS, with the exception of 2-methyl-1-propansulfonic acid functionality. Therefore, it was assumed that the presence of AAm contributes some distance among the sulfonyl groups acting as spacer and provides control over particle size. The effect of copolymer composition on particle size and metal ion loading capacity will be reexamined.

Thermal and structural evaluations

The nature of the particles in the network and the metal loading capacity and the crystalline structure of the metal particles were investigated by means of TGA and wide-angle XRD measurements, respectively. Figure 4 presents the bulk and iron particle-loaded 0.75% X p(AMPS) (a) and c-p(AMPS) (b) hydrogel thermograms. The thermograms were obtained under N_2 atmosphere to prevent oxidation of metal particles by first heating up to 100 °C and keeping there for 30 min for dehydration and then cooling back to 35 °C and followed by ramping up to 1,000 °C with 10 °C/min heating rate. The weight loss with time was recorded as shown in the figure. The bulk 0.75% X p(AMPS) hydrogel showed multidegradation temperature approximately around 142, 195, 240, 315, and 430 °C, whereas its c-p (AMPS) hydrogels showed only one sharp degradation temperature at about 368 °C. For the other hydrogels, 0.5% and 1% X, quite analogous thermal behavior was observed (data are not shown). The sharp degradation temperature around 368 °C is the most prominent feature of different % cross-linked c-p(AMPS) hydrogels, implying the strong attachment of iron particle to the hydrogel network. This is conceivable since metal particles grow on and around the neighboring functional groups, which is accountable for metal ion absorption, of polymer chains, they can enclose some polymer chains in their crystalline lattice during the growth period. Another noticeable characteristic of the metal particle is their almost spherical dendrite shape as illustrated in Fig. 5a. The individual iron particle shown in Fig. 5a has a polymer network around and through it (haze in the TEM images) confirming the strong attachment. In addition, leakage of iron particles from the swollen hydrogels in water was not seen in the shaker at room temperature for a week. Due to the localized metal ions, which are electrostatically hindered by the opposite charges on polymer network (constrained environment), interfacial free energy favors spherical particles. In other words, surface energy is the lowest for spherical particles or the

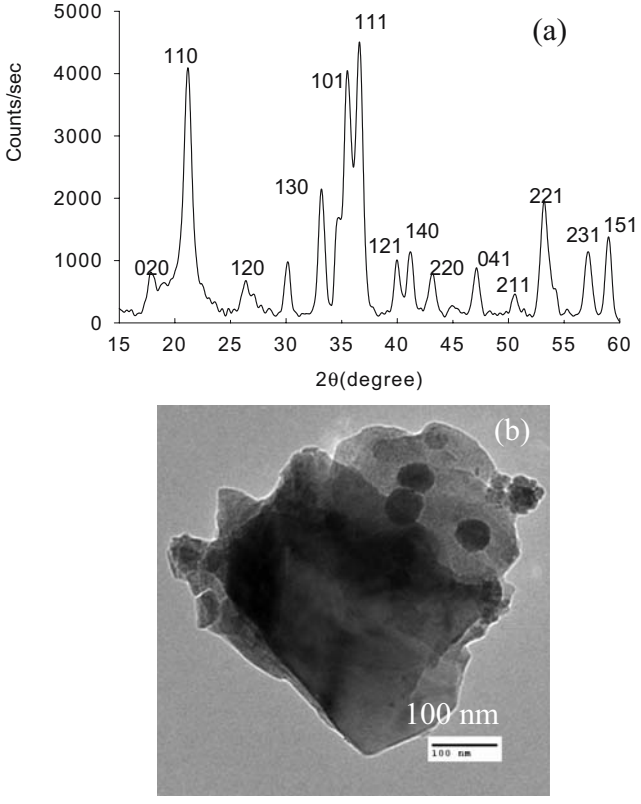

Fig. 6 **a** XRD data of 0.75% X c-p(AMPS). **b** TEM images of iron-loaded 50:50 (mole ratio) of 1% X c-p(AMPS-c-AAm) hydrogel

energy is proportional to the surface area and sphere has the lowest area for a given volume. Again, from Fig. 4, heating up 1,000 °C, bulk p(AMPS) hydrogel almost completely degraded (~99%), whereas iron-loaded c-p(AMPS) hydrogels lost ~75% of its original weight. For 0.5% and 1.0% X-ed hydrogels, quite similar results were obtained. Therefore, it can be said that the loading of metal particle for these hydrogel networks is quite high, approximately 20–30% by weight, which was achieved on a single absorption and reduction cycle bearing in mind that further loading of metal ions by multiple cycles of absorption reduction procedures is also possible. Wang et al. [27] prepared polyelectrolyte multilayers made up of poly

Table 1 TGA evaluation of iron-loaded 0.5% X c-p(AMPS-c-AAm) hydrogel

AMPS/AAm mole ratio	% Weight loss		Degradation temperatures (°C)	
	600 (°C)	1,000 (°C)		
1.0:0.0	47	73	339 (391)	661
0.75:0.25	48.3	77.8	352	665
0.50:0.50	50.4	83	357.7	675
0.25:0.70	54.1	87.6	(277.4) 390.8	–
0.0:1.0	87.1	95.3	(240) 366	–

(acrylic acid) (p(AAc)) and poly(allyamine hydrochloride) (p(AH)) and used as nanoreactor for silver nanoparticle composite preparation. They have demonstrated the manipulation of silver nanoparticle size and overall silver concentration by controlling the pH of multilayer assembly and by repeatedly incorporating silver through cycles of ion exchange and reduction processes. In some application such as hyperthermia, magnetic particle content of devices is very important for therapy purposes [19]. Figure 5b denotes the magnetic property of iron-loaded 0.75% X c-p(AMPS) hydrogels, obtained via VSM measurements. As depicted in Fig. 5b, after magnetization, it has a room temperature magnetization of ~0.4 emu/g of composite material at ~5 kOe as determined by VSM. The absence or very little hysteresis at room temperature suggests almost superparamagnetic behavior in consistent with the small particle size of iron oxide particles; therefore, the composite material is ferromagnetic in nature. The XRD data given in Fig. 6a were taken by grinding the fine powdered freeze-dried c-p(AMPS) hydrogels with Siemens Diffraktometer at the angle (2θ) between 10 and 60 degrees. The XRD data were confirmed as FeO(OH) in comparison with XRD data bank from the literature and *d*-spacing values, and the corresponding miller indices of matching peaks were shown on the graph.

The possibility of controlling the metal particle size by preparing copolymeric hydrogels of AMPS with AAm was further investigated. Figure 6b is the verification of particle size control with AMPS content. This figure illustrates the TEM images of 1% X 50:50 AMPS/AAm mole ratio of iron-loaded c-p(AMPS-c-AAm) composite material. The particles are about 40 nm; however, further decrease in the amount of AMPS did not lead to reasonable smaller, well-defined particles with homogenous features, but rather, it causes relatively smaller particles with broad size distribution 2–15 nm (figures are not shown) suggesting the random distribution of the functional groups for metal ion absorption and particle formation. Although both monomers have (AMPS and AAm) very similar chemical structure and most of the AAm derivatives have close reactivity ratios [28], they would not yield perfectly alternating copolymeric structures and AAm can afford some distance among the metal ion absorbed functional

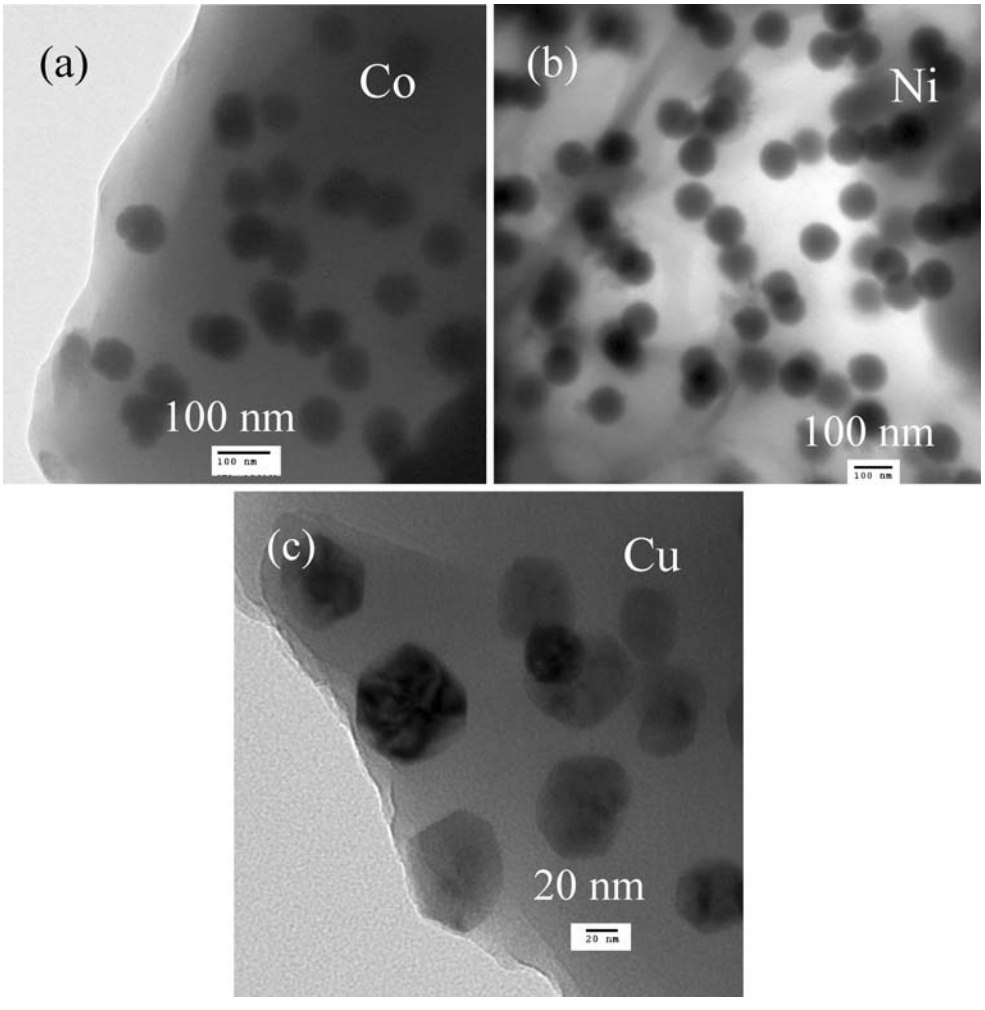

Fig. 7 TEM images of 0.75% X p(AMPS) hydrogels loaded with Co (**a**), Ni (**b**), and Cu (**c**)

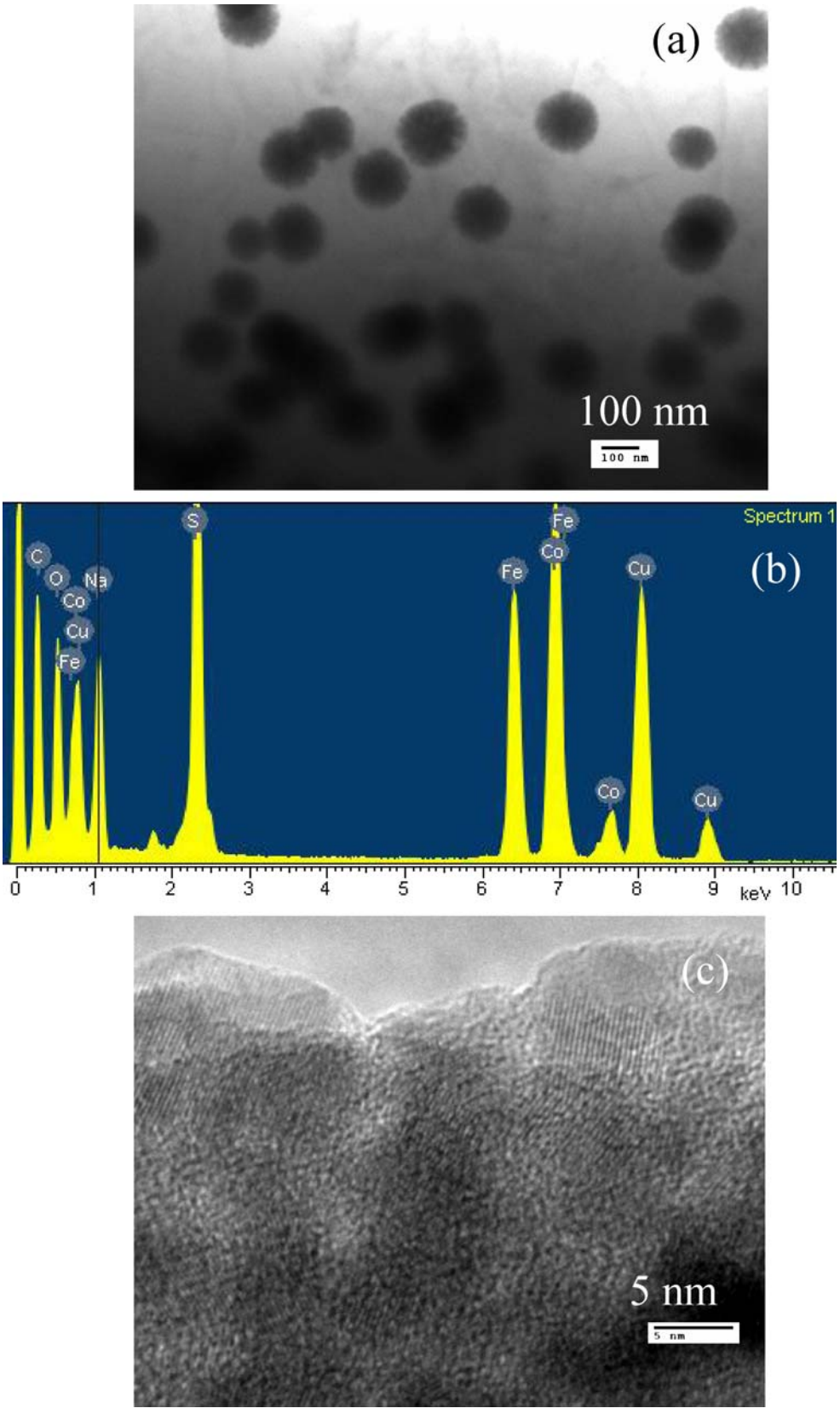

Fig. 8 (**a**) TEM images 0.75 % X c-p(AMPS) hydrogels containing Fe/Co metal alloy nanoparticles (1:2 mole ratio). (**b**) Elemental analysis results of same alloy (EDAX). (**c**) TEM images of CdS quantum dots containing c-p(AMPS) hydrogel

groups for metal particle formation resulting in irregular and wide particle size distribution.

Table 1 shows the results of TGA evaluations of iron-loaded 0.5% X p(AMPS-c-AAm) copolymeric hydrogel prepared in different mole ratios. It was observed that degradation temperatures shift a few °C depending on the extent of AAm in the copolymer structure. As can be seen from the table, metal ion loading decreases with the increase in the amount of AAm in the hydrogel networks, with heating up to 1,000 °C varying from ~30% to 5% by weight. This can be explained by the fact that the functional groups, which are responsible for metal ion absorption, come from AMPS monomer, and the lesser the amount of those functional groups, the smaller the amount of iron loading. Another noticeable characteristic for the copolymeric networks is the degradation temperatures. Initially, the two degradation temperatures at 343 and 653 °C (which was not significant for 0.75% X c-p(AMPS)) increase with the amount of AAM content up to 0.5:0.5 mole ratio. For hydrogels containing more than 50% AAm, another lower degradation temperatures were seen around 277 and 240 °C for 0.25:0.75 and 0.0:1.0 mole ratios of AMPS/AAm, respectively. In addition, sharp, distinct higher degradation temperatures were disappeared (more than 600 °C) due to the different structures of both components replacing broader range of degradation temperature. Although it was shown in Fig. 4b that there is only one sharp degradation temperature at around 368 °C for 0.75% X c-p(AMPS) hydrogel, 1% X c-p(AMPS) gel gives rise to one sharp peak at 343 °C and a small degradation around 388 °C; this could be attributed to the less homogeneities in the network structure at higher cross-linker contents.

In addition to iron particles, other metal particles were also prepared by employing the same procedure, for example, by absorbing Co, Ni, and Cu ions from their salt solution (0.1 M) and followed by reduction step with $NaBH_4$. The prepared samples of TEM images are shown in Fig. 7a–c, respectively. Depending on the types of metal ions, different shape and the morphology of particles can be obtained. Even metal alloys can be prepared by simultaneously absorbing the two metal ions (iron and cobalt at 1:2 mole ratios) from their ion solution mixtures and by reducing with the same procedure described above. The TEM image of such particle system is shown in Fig. 8a, which reveals the particle size about 100 nm, and the elemental analysis result confirms that almost 1:2 mole ratio can be attained as was the feed ratio (Fig. 8b and Table 2). Here, cobalt is chosen as co-ion for alloy nanoparticle preparation because cobalt is also known with its magnetic properties for various applications. Furthermore, CdS quantum dots can also be prepared by utilizing the same procedure. After contacting Cd^{2+}-loaded p(AMPS) hydrogels with S^{2-} containing aqueous solution, a bright yellow color was appeared throughout the hydrogel matrix as an indication of CdS quantum dots formation. Figure 8c illustrates the TEM images of CdS quantum dots with the crystal lattice size range of around 5 nm. The details of these other metal particles, their alloys, and quantum dots are currently under investigation.

Table 2 The composition of Fe/Co alloy obtained by elemental analysis of 0.75% X c-p(AMPS)

Element	Wt.%	At.%
FeK	34.70	35.93
CoK	65.30	64.07
Total	100.0	

Conclusions

Inorganic nanoparticle syntheses in the confined environment of polymeric templates such as hydrogel three-dimensional matrixes have shown to be very useful for the preparation of composite materials with additional functionalities such as magnetic field sensitivity. In this study, it was demonstrated that the magnetic iron particle synthesis inside a pH-sensitive hydrogel utilizing the ion exchange feature of hydrogel network can be accomplished by adsorbing the metal ion precursor from its solution and by reducing with appropriate reducing agent. It was observed that cross-linker density has no prominent effect on particle size, whereas the ion exchange capacity plays a major role on the size and the loading capacity of the inorganic material. The ion exchange capacity of matrix material (AMPS) was very high (20–30 wt%) and can be tuned by synthesizing copolymeric hydrogel absorbents containing various amounts of functional group. It was also demonstrated that other kinds of metal particles such as Ni, Co, and Cu as well as alloys can also be prepared utilizing the same procedure. In summary, the used p(AMPS) hydrogel is a very good choice of template material for in situ inorganic nanoparticle synthesis with potentially well-defined characteristics and morphology for biomedical application. These types of templates based on three-dimensional synthetic hydrogels are attractive alternatives to nonaqueous system with the advantage of being compatible with biological molecules, cells, and tissues [29, 30]. In fact, the current research is focused on the precise control of the size of the different nanometals including semiconductor formation inside the micro/nano-hydrogels for diverse applications. These materials have great potential in biomedicine such as catalysts, (bio) sensors, hyperthermia applications, switchable electronic, and signal-triggered delivery systems.

Acknowledgments The author is grateful to Prof. Dr. Vijay T. John for providing great contribution to the work. Also, acknowledges go to TIMES (Tulane Institute for Macromolecular Engineering and Science), Prof. Dr. Tarun Mandal from Xavier University for SEM images, and UNO (University of New Orleans) for VSM measurements.

References

1. Landfester K (2001) Adv Mater 13:765
2. Kane SR, Cohen ER (1999) Chem Mater 11:90
3. Joly S, Kane R, Radzilowski L, Wang T, Wu A, Cohen ER, Thomas LE, Rubner FM (2000) Langmuir 16:1354
4. Dante S, Hou Z, Risbud S, Stroeve LP (1999) Langmuir 15:2176
5. Dai J, Bruening LM (2002) Nano Lett 2:497
6. Ménager C, Sandre O, Mangili J, Cabuil V (2004) Polymer 45:2475
7. Bekiari V, Pagonis K, Bokias G, Lianos P (2004) Langmuir 20:7972
8. Peppas A N, Leobandung WJ (2004) Biomater Sci Polymer Edn 15:125
9. Mandracchia D, Pitarresi G, Palumbo BS, Carlisi B, Giammona G (2004) Biomacromolecules 5:1973
10. Xulu PM, Filipcsei G, Zrínyi M (2000) Macromolecules 33:1716
11. Flynn L, Dalton PD, Shoichet MS (2003) Biomaterials 24:4265
12. Song J, Saiz E, Bertozzi CR (2003) J Am Chem Soc 125:1236
13. Hu Y, Chen J, Chen W, Ning J (2004) Mater Lett 58:2911
14. Chaggar RS, Hall AJ, Miller JD (1996) Polymer 37:5313
15. Kroll E, Winnik FM (1996) Chem Mater 8:1594
16. Pardo-Yissar V, Gabai R, Shipway AN, Bourenko T, Willner I (2001) Adv Mater 13:1320
17. Shipway AN, Willner I (2001) Chem Commun 20:2035
18. López D, Cendoya I, Mijangos C (2001) Macromol Symp 166:173
19. Lao L, Ramanujan VR (2004) J Mater Sci Mater Med 15:1061
20. Chatterjee J, Haik Y, Chen CJ (2003) Colloid Polym Sci 281:892
21. Juliac E, Mitsumata T, Taniguchi T, Iwakura K, Koyama K (2003) J Phys Chem B 107:5426
22. Sauzedde F, Elaïssari A, Pichot C (1999) Colloid Polym Sci 277:846
23. Gu S, Shiratori T, Konno M (2003) Colloid Polym Sci 281:1076
24. Takafuji M, Ide S, Ihara H, Xu Z (2004) Chem Mater 16:1977
25. Zhang J, Coombs N, Kumacheva E, Lin Y, Sergant EH (2002) Adv Mater 14:1756
26. Xu S, Zhang J, Paquet C, Lin Y, Kumacheva E (2003) Adv Funct Mater 3:468
27. Wang TC, Rubner MF, Cohen RE (2002) Langmuir 18:3370
28. Brandrup J, Immergut EG, Grulke EA (1999) Polymer handbook, 4th edn. Wiley, New York
29. Wang C, Flynn NT, Langer R (2004) Adv Mater 16:1074
30. Kato N, Oishi A, Takahashi F (1998) Mater Eng C 6:291